BUTTERWORTH HEINEMANN

Polymer Vol. 36 No. 23, pp. 4379–4384, 1995

0032-3861/95/$10.00+0.00

Modelling of time dependence in ultra-high-modulus polyethylene based on Raman microscopy

A. Sengonul and M. A. Wilding*
Department of Textiles, UMIST, PO Box 88, Manchester, UK
(Received 24 October 1994)

Previous research dealt with the modelling of time dependence in ultra-high-modulus polyethylene in terms of mechanical systems. Although such attempts were highly successful in describing time-related phenomena in melt-spun polyethylene, they were less able to account for the behaviour of gel-spun material. Moreover, in the early experiments, only the *macroscopic* deformation could be determined. Recent advances in Raman microscopy have enabled a study of the changes in *internal* strain associated with crrep and recovery. This short paper considers some preliminary creep data in terms of mechanical models which, despite their simplicity, are nevertheless able to provide a phenomenological basis for a number of the observed features: most notably the attainment of a strain maximum in one of the differently stressed structural components.

(Keywords: high-modulus polyethylene; Raman microscopy; creep modelling)

INTRODUCTION

The medium- and long-term applications of ultra-high-modulus polyethylene (UHMPE) continue to be limited by its susceptibility to creep and stress relaxation. Previous studies[1–5] examined these phenomena over a range of conditions and chemical modifications, and yielded some success in the development of appropriate models. The response to stress or strain was envisaged as arising from two viscoelastic/plastic processes acting in parallel, and associated respectively with highly aligned crystalline and network fractions. Experimental data agreed well with this model, or with close variants of it, for melt-spun-then-drawn filaments, although the results for gel-spun fibres suggested a difference in kind between the two types of material. In these early studies it was not possible to determine directly the variation of response *within* the fibre structure.

Advances over recent years in the use of Raman microscopy to study deformation micromechanics have provided us with a means of testing the validity of the modelling with greater rigour.

This short paper considers some of the past successes in the modelling of relaxation phenomena in UHMPE, and introduces preliminary attempts, using Raman microscopy, to interpret creep/recovery data on gel-spun filaments in terms of viscoelastic models similar to, but distinct from, those previously developed.

HISTORICAL

Models of time dependence in melt-spun UHMPE

Research carried out during the late 1970s and early 1980s[1,2] produced limited success in describing the viscoelastic and plastic behaviour of melt-spun UHMPE using standard combinations of Maxwell and Voigt elements. However, these highly simplistic systems were unable to account for the considerable non-linearity observed in the stress response. Subsequent publications[3–5] viewed the time dependence in terms of two stress-assisted thermally activated rate processes, coupled with associated elastic elements, acting in parallel. The rate processes were assumed to be of the type originally proposed by Eyring[6] for certain flow phenomena. In melt-spun UHMPE, the flow processes were thought of as arising from deformation mechanisms within a continuous crystalline fraction, and a highly aligned, parallel amorphous network, respectively. The activation parameters derived for one of these processes were consistent with a localized event, such as the propagation of a Reneker defect through the continuous crystal phase[7].

Model 1. The essential features of the model referred to above ('Model 1' in the present notation) appear in *Figure 1*. This model can be analysed for the steady-state creep condition (plastic flow, or 'secondary' creep) in which both springs have attained their ultimate extension, in order to study stress dependence. It was found to apply extremely well for many molecular-weight grades of UHMPE (which included certain copolymers and lightly radiation-crosslinked samples), and over a wide range of applied stress levels and temperatures.

Figure 2 presents some examples, taken from ref. 5, of the fits to the data that were achieved using Model 1. In this diagram the equilibrium strain rate is plotted as a function of the applied stress, and the full curves are calculations based on the model.

* To whom correspondence should be addressed

Model 1

a) equilibrium creep:

$$\varepsilon_p' = [\varepsilon_0']_1 \sinh \{\sigma_1 v_1/kT\} = [\varepsilon_0']_2 \sinh \{\sigma_2 v_2/kT\}$$

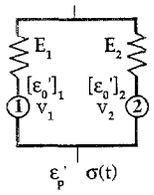

b) stress-relaxation:

$$\sigma_1(t) = \{2kT/v_1\} \operatorname{arctanh} \{\exp[(\gamma_1\delta_1 - t)/\gamma_1]\}$$

$$\sigma_2(t) = \{2kT/v_2\} \operatorname{arctanh} \{\exp[(\gamma_2\delta_2 - t)/\gamma_2]\}$$

$$\sigma(t) = \sigma_1(t) + \sigma_2(t)$$

where γ and δ are functions of T, and the appropriate activation parameters.

Model 1a

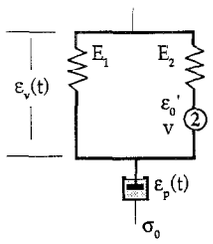

Total creep response:

$$\varepsilon'(t) = \varepsilon_v'(t) + \varepsilon_p' = \{E_2/(E_1+)\}\, \varepsilon_0' \sinh \{[\sigma_0 - \varepsilon_v(t)\, E_1]\, v/kT\} + \varepsilon_p'$$

Figure 1 Models for relaxation phenomena in melt-spun UHMPE[3–5]

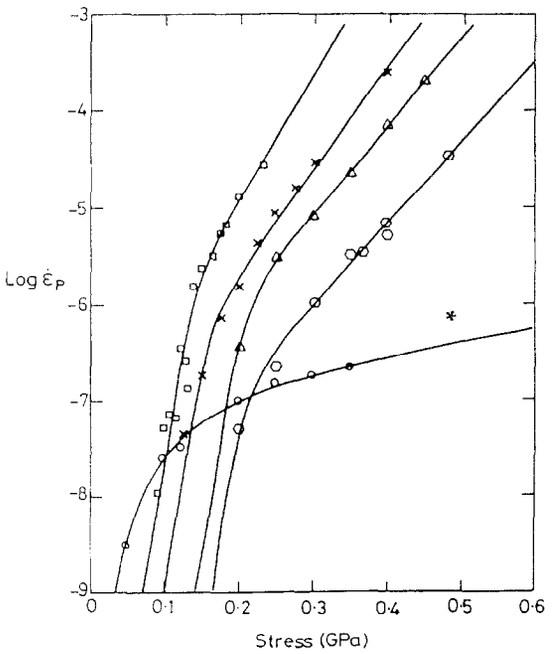

Figure 2 Curves fitted to equilibrium creep strain rate vs. applied stress data at 20°C on the basis of Model 1 for a range of UHMPE grades[5]. The curve marked by a star (*) belongs to a gel-spun sample

The principal disadvantage of Model 1 lay in the fact that its analysis for conditions of non-equilibrium creep is far from straightforward. It is not possible, for example, to derive separate values for the two spring constants under steady flow conditions. On the other hand, the model may readily be analysed in the stress-relaxation mode.

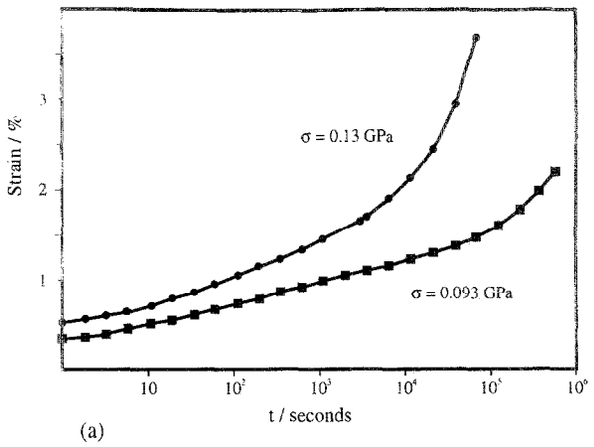

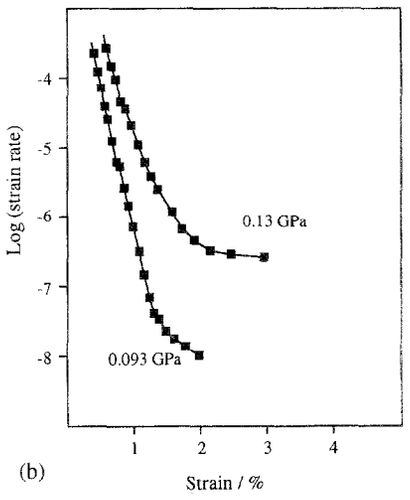

Figure 3 Creep data (symbols) compared with fitted function (full lines) on the basis of Model 1a for Rigidex 50, draw ratio 20×, at 20°C at two applied stress levels: (a) total creep strain against log(time); (b) log(strain rate) against strain[4]

Model 1a. *Figure 1* includes a variant of Model 1, referred to here as 'Model 1a'. The activation parameters deduced for Model 1 are such that for any given (moderate) applied stress, and over a reasonable timescale, Model 1a becomes formally equivalent to Model 1. Since Model 1a may be analysed for conditions of non-equilibrium creep (i.e. the viscoelastic regime), this enabled estimates to be made of E_1 and E_2. *Figure 3* presents examples, taken from ref. 4, of the excellent agreement obtained between experimental and calculated data. In *Figure 3a* creep strain is plotted against log(time) for a medium-molecular-weight grade at two applied stress levels. *Figure 3b* presents the results in the alternative format of log(strain rate) vs. strain, which was demonstrated by Sherby and Dorn[8] to be a useful means of identifying the onset of plastic flow (the so-called 'plateau strain rate').

The values of the spring constants derived from the fitting of Model 1a to creep data were fed back to the original Model 1, to be tested against stress-relaxation data. This provided an independent check on the general validity of the modelling approach, and *Figure 4* compares predicted and actual stress-relaxation data[4] for the sample shown in *Figure 3*.

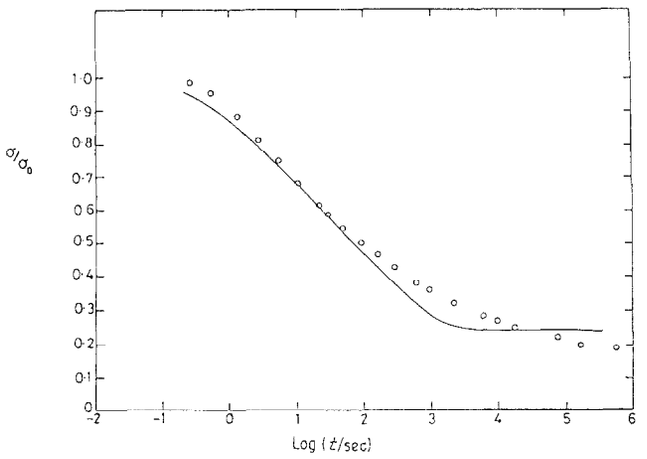

Figure 4 Stress-relaxation curve for Rigidex 50, draw ratio 20×, at 20°C. The full curve is predicted, based on Model 1 using values of E_1 and E_2 derived from fitting Model 1a to non-equilibrium creep data. The activation parameters were those derived from fitting Model 1 to equilibrium creep[4]

A shortcoming of both Models 1 and 1a was that they evidently did not apply well to gel-spun polyethylene, whose behaviour appeared to differ in kind from that of the melt-spun materials. Although a fit could be obtained for gel-spun UHMPE (see *Figure 2*), this was only possible using quite different, and seemingly unrealistic, values for the model parameters.

CREEP MONITORED BY RAMAN SPECTROSCOPY

The Raman 'strain gauge'

The Raman spectrum of UHMPE contains several stress-sensitive bands. Young *et al.*[9] investigated a similar feature in other stiff fibre types (such as the aromatic polyamide Kevlar), and deduced that the Raman shift was linearly related to strain to the extent that the effect could be calibrated to provide a microscopic 'strain gauge', by which internal micro-strains/stresses could be monitored.

A number of authors (for instance refs. 10–13) have used essentially the same technique to study deformation micromechanics in high-modulus polyethylene. Attention centred on the strain sensitivity of a particular compound band, arising from the symmetrical C–C stretching mode near 1130 cm^{-1}. This system displays a narrow component and a less intense, broad component. Both components show shifting of frequency with applied stress and with time, but the broad component is significantly more sensitive than the narrow. These two components are considered to correspond to differently stressed groups of C–C bonds within two distinct structural environments. There is also an effect on the bandwidths, which suggests changes in the distribution of load-bearing bonds in each environment during deformation.

Figure 5 illustrates the effect on the band structure of applying a strain of 4% to a polyethylene filament[13]. Recently, other researchers[13,14] have used the stress sensitivity of the Raman spectrum of polyethylene to examine time-related phenomena, although no attempt was made to model the effects.

In the present work, gel-spun UHMPE filaments have been creep tested whilst mounted under a Raman microscope. The results were monitored in terms of shifts in the peak positions of the broad and narrow band components with time. During creep under a positive external tensile stress, the macroscopic strain and strain rate *must both be positive* (or possibly zero). During recovery, the strain rate will be negative, but again the macroscopic strain can only be positive or zero. The response as detected by the Raman technique is more complex: in particular, it appears that, even during the loading period, the individual strain components can pass through a maximum (followed by negative strain rate). As will be demonstrated, it is possible to account for this observation in a phenomenological way, using a relatively straightforward system of springs and dashpots.

During recovery, the 'Raman strains' may be extensional immediately after unloading, but both quickly pass through zero into compression before ultimately decaying. This behaviour is impossible to account for using a simple two-process system, since an additional parallel element is required to provide the necessary compression. Some authors[10] have in fact postulated the existence of a third, differently stressed, region. It is possible that this component is not detected by the Raman technique.

Experimental

Material. The material studied was a gel-spun ultra-high-molecular-weight polyethylene multifilament yarn supplied by DSM Research. These fibres are characterized by high tenacity and high degrees of orientation

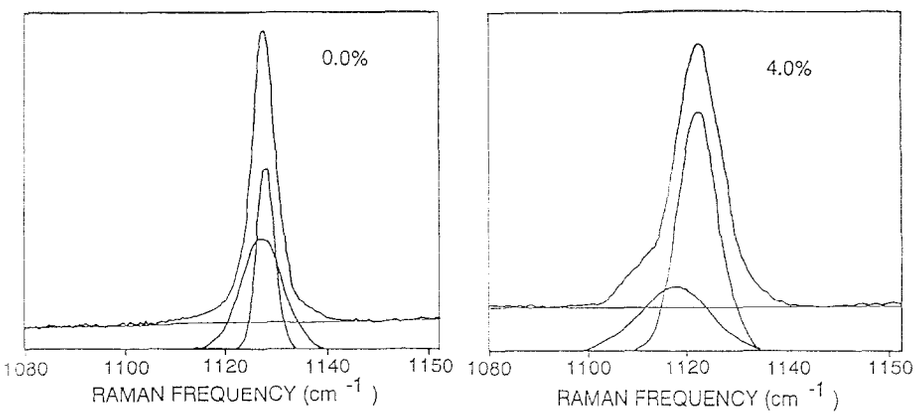

Figure 5 Structure of the composite Raman band near 1130 cm^{-1}, and the effect of applying a macroscopic strain of 4%[13]

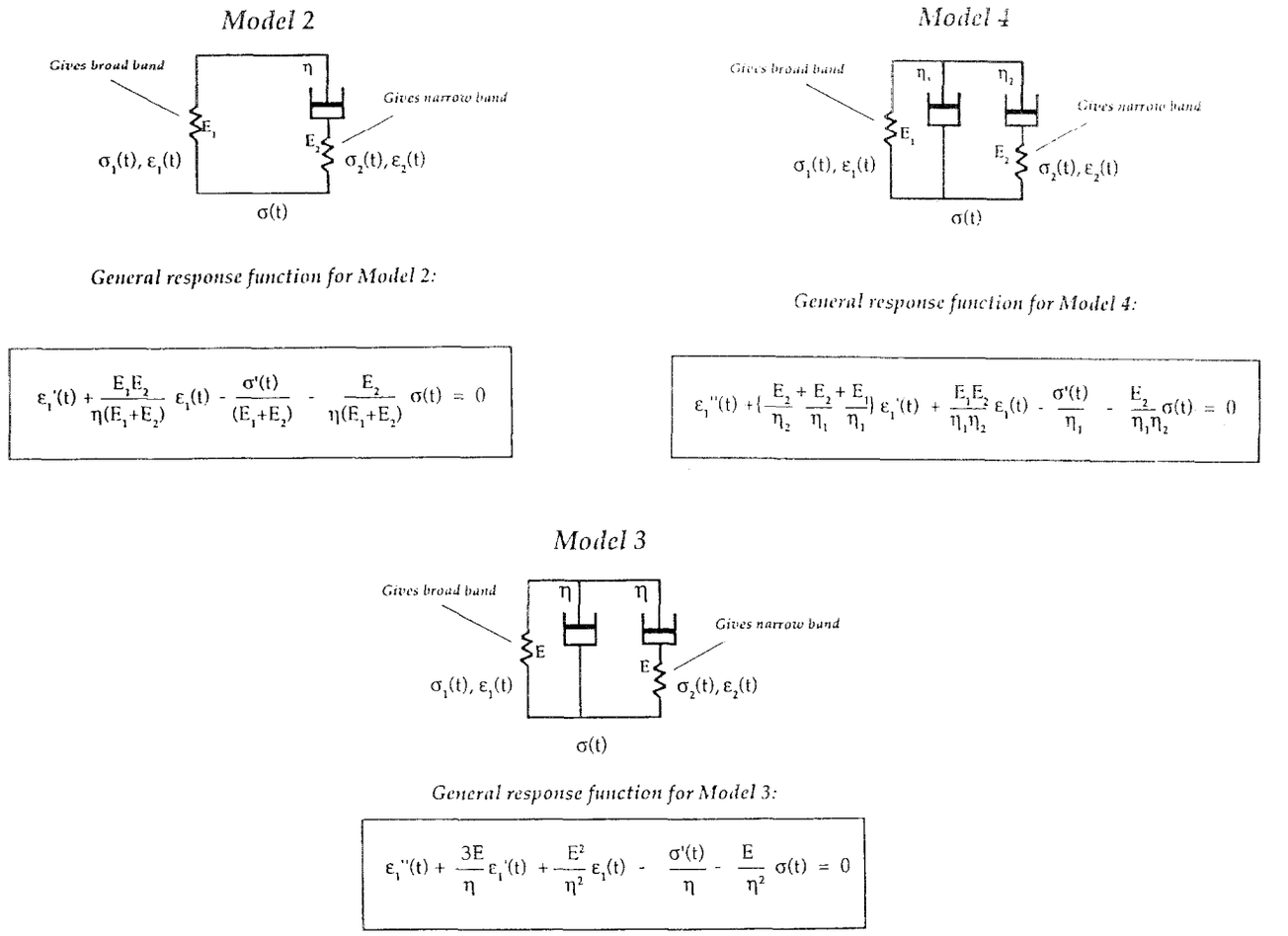

Figure 6 Models for time dependence in gel-spun polyethylene

and crystallinity. This was also confirmed by us from wide-angle X-ray diffraction measurements.

It was not possible to quantify the single-filament cross-section directly, owing to the highly irregular profile, which in places was almost bean-shaped. However, optical measurements suggested an effective diameter of approximately 12.74 μm (taking the mean of the major and minor axes). The linear density of the single filaments was calculated as 0.114 tex from the manufacturer's specification. Using the quoted density of 970 kg m^{-3}, this gives a diameter of 12.3 μm for an equivalent circular filament, which compares favourably with the microscopic estimate.

Instrumentation. The Raman spectra were recorded using a Spex 1403 double monochromator employing a modified Nikon optical microscope. The detection system comprised a cooled charge-coupled device (c.c.d.) camera. This enabled a complete scan to be made of the appropriate spectral region every 50 s.

The excitation source was the 488 nm line of an argon-ion laser operating at 20 mW. The incident radiation was focused to a spot size of 2 μm.

Procedure. Single-filament samples for investigation were mounted on a small loading jig placed on the stage of the Raman microscope. Timing of each test was initiated simultaneously with the application of the appropriate tensioning weight. The first Raman spectrum was recorded after a period of 120 s, with subsequent spectra being recorded at intervals of 120 s. A total creep period of 600 s was allowed, followed by a period of recovery.

The experiment was replicated at three levels of applied tension, using a fresh sample for each. The equivalent tensile stresses were: 0.778, 1.156 and 1.546 GPa.

Modelling of creep in gel-spun polyethylene, and Raman results

If it can be assumed that there is a linear relationship between the microscopic strain in a C–C bond and the corresponding vibrational frequency, and further that the Raman shift vs. strain sensitivity factor ($d\tilde{\nu}/d\epsilon$) is the same —and known—for both types of C–C bond, then the relative strains in each structural region can be inferred from the Raman data. Conversely, from a proposed mechanical model of creep, it is possible to simulate curves of 'Raman shift' vs. time for the two components. We have used the value of 800 cm^{-1} per unit strain quoted by previous workers for a pure PE crystal[12], although a precise knowledge of this factor is not necessary in order to assess the general validity of any particular model. It is assumed that amorphous fractions do not contribute to the structure of the observed Raman band.

We have been able to interpret the creep behaviour of gel-spun polyethylene in terms of surprisingly simple

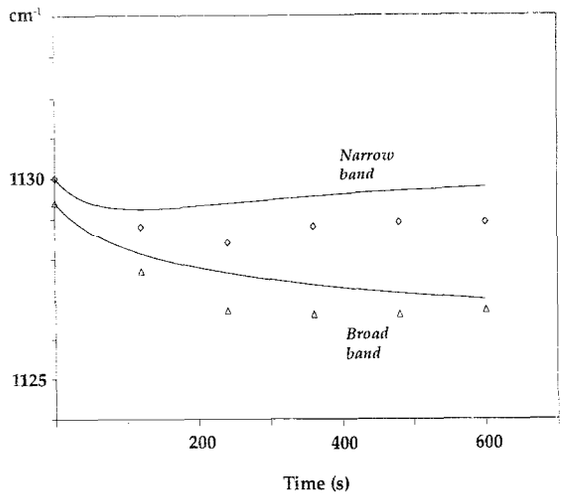

(a)

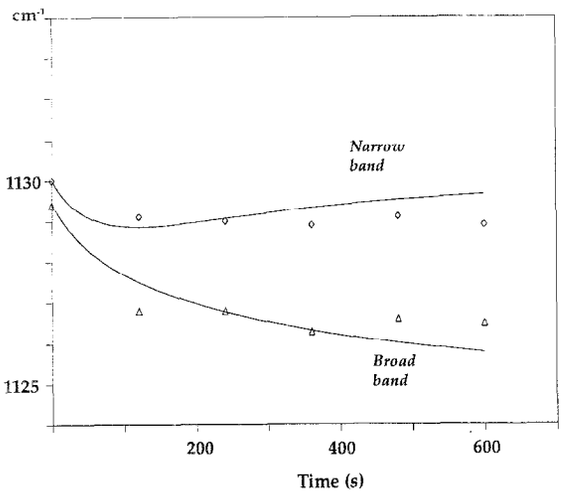

(b)

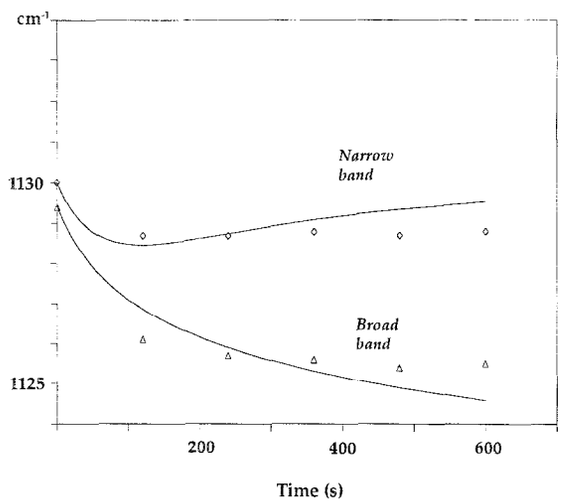

(c)

Figure 7 Comparison of recorded Raman shift vs. creep time data for gel-spun sample (symbols) with simulated shifts (full curves) based on Model 3. Applied stress: (a) 0.778 GPa; (b) 1.156 GPa; (c) 1.546 GPa. Fitted parameters: $E = 220$ GPa, $\eta = 3 \times 10^{13}$ P

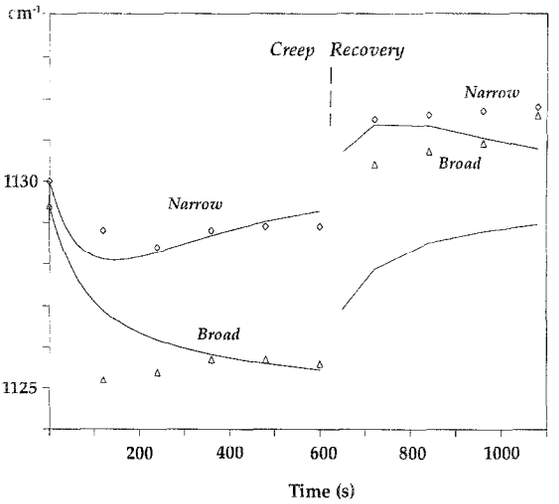

Figure 8 Comparison of recorded Raman shift vs. creep and recovery time data for gel-spun sample (symbols) with simulated shifts (full curves) based on Model 4. Applied stress: 0.778 GPa. Fitted parameters: $E_1 = 140$ GPa, $E_2 = 60$ GPa, $\eta_1 = \eta_2 = 1.5 \times 10^{13}$ P

models. These are illustrated in *Figure 6*, which also indicates the general differential equation that must be solved in each case. This is a relatively straightforward procedure requiring a knowledge of the appropriate boundary conditions for creep and recovery. Model 2 is in fact the standard linear solid. Models 3 and 4 provide additional damping, represented by the second dashpot. Model 3 is the simplest case of the more general Model 4, and assumes two identical springs and two identical dashpots. All three models predict the development of negative (compressional) strain in the right-hand spring during recovery. Models 3 and 4 further predict that the strain in the right-hand spring should pass through a maximum at some point during the creep stage. The left-hand spring should mirror the macroscopic creep/recovery strains.

Figure 7 shows Raman frequency vs. creep time plots at three stress levels. The symbols are recorded data, while the full curves are calculated from Model 3 using the parameters indicated. Model 4 provides flexibility over and above Model 3, and *Figure 8* shows creep and recovery data for one of the applied stress levels. Again, the symbols are recorded data, while the full curves are calculated from the model using the indicated parameters. No systematic attempt has so far been made to optimize the parameters for either Model 3 or 4, and the values chosen were arrived at by visual trial and error.

DISCUSSION AND CONCLUSIONS

Over the limited range of testing conditions used so far, Models 3 and 4 describe the observed creep behaviour qualitatively well, despite their simplicity (most notably the fact that the dashpots are Newtonian, whereas the materials originally studied[1–5] showed considerable stress non-linearity). An important result is the prediction of a strain maximum in one of the two components during the loading period. Significantly, Models 3 and 4 are consistent with the scheme proposed elsewhere (and arrived at independently) for the distribution of crystalline fractions within the gel-spun structure[10–12].

Moreover, our values for the spring constants are in broad agreement with theoretical estimates of the pure crystal modulus (ca. 200 GPa), adding further weight to the general validity of the modelling.

The recovery results are less well modelled, however: it is notable that the recorded data show a positive frequency shift of both band components shortly after unloading. This is indicative of compressive strains occurring simultaneously in *both* of the identified structural regions. None of the models proposed here allows compressive strains in both springs simultaneously under conditions of zero external stress. Clearly, it will be necessary to refine these models in an attempt to account for this rather unusual feature. Further, it is likely that a more satisfactory representation of the creep behaviour could be achieved by replacing the simple Newtonian dashpots with Eyring flow processes. The work is as yet at a preliminary stage, and more experimental data will be needed to clarify the situation. The next phase of the work will address these and other aspects, such as temperature dependence.

ACKNOWLEDGEMENTS

The authors wish to express their thanks to Mr M. J. N. Jacobs, of DSM High Performance Fibers BV, Heerlen, The Netherlands, for providing the yarn samples studied. We are also indebted to Professor R. J. Young, of the Manchester Materials Science Centre, for use of the Raman microscope and for valuable discussions.

REFERENCES

1 Wilding, M. A. and Ward, I. M. *Polymer* 1978, **19,** 969
2 Wilding, M. A. and Ward, I. M. *Polymer* 1981, **22,** 870
3 Wilding, M. A. and Ward, I. M. *Plast. Rubber Process. Appl.* 1981, **1,** 167
4 Wilding, A. M. and Ward, I. M. *J. Mater. Sci.* 1984, **19,** 629
5 Ward, I. M. and Wilding, M. A. *J. Polym. Sci., Polym. Phys.* 1984, **22,** 561
6 Eyring, H. *J. Chem. Phys.* 1936, **4,** 283
7 Reneker, D. H. *J. Polym. Sci.* 1962, **59,** 539
8 Sherby, O. D. and Dorn, J. E. *J. Mech. Phys. Solids* 1956, **6,** 145
9 Young, R. J., Lu, D. and Day, R. J. *Polym. Int.* 1991, **24,** 71
10 Kip, B. J., Van Eijk, M. C. P. and Meier, R. J. *J. Polym. Sci., Polym. Phys.* 1991, **29,** 99
11 Mioonen, J. A. H. M., Roovers, W. A. C., Meier, R. J. and Kip, B. J. *J. Polym. Sci., Polym. Phys.* 1992, **30,** 361
12 Wong, W. F. and Young, R. J. *J. Mater. Sci.* 1994, **29,** 520
13 Wong, W. F. and Young, R. J. *J. Mater. Sci.* 1994, **29,** 510
14 Grubb, D. T. and Li, Z. F. *Polymer* 1992, **23**(12), 2587